Austin Journal of Clinical Neurology

Open Access

Austin Publishing Group

Research Article

Lactate May Reduce Aβ42 through Activating GPR81-PI3K/Akt/CREB-DNMT1 Signaling Pathway in APP/PS1 Mice

Zhang M, Wang Y, Guan X, Chen X, Ge G and Guo H*

Department of Medical Genetics, College of Basic Medical Sciences, Army Medical University, 30 Gaotanyan Main Street, Shapingba District, Chongqing 400038, China

***Corresponding author**: Hong Guo, Department of Medical Genetics, College of Basic Medical Sciences, Army Medical University, 30 Gaotanyan Main Street, Shapingba District, Chongqing 400038, China

Tel: +86-13452334616;

Email: guohong02@tmmu.com

Received: May 11, 2025

Accepted: June 05, 2025

Published: June 09, 2025

Abstract

Lactate provides signals that modulate neural functions, including excitability, plasticity and memory consolidation. G-protein-coupled receptor 81 (GPR81) is a specific receptor of lactate, which functions in signaling regulation in neural activity. This process is mediated by downstream of GPR81, phosphatidylinositol 3 kinase /protein kinase B/cyclic adenosine monophosphate response element binding protein (PI3K/Akt/CREB) pathway. Previously, it is recognized that lactate content is reduced in the brain of Alzheimer's disease (AD) model mice. But, it hasn't been identified whether lactate decrease is related with increased amyloid beta (Aβ) burden in AD model mice. We examined cerebral lactate content and expressions of GPR81, p-PI3K, p-Akt, p-CREB in wild type and double-transgenic amyloid precursor protein/presenilin 1 by performing immunostaining and western blotting (WB), and identified expressions of deoxyribonucleic acid methyltransferase 1 (DNMT1), beta-site amyloid precursor protein cleaving enzyme 1 (BACE1), and Aβ burden in wild type and APP/PS1 mice. To investigate lactate involved in Aβ burden of AD, we performed Thioflavin S (Th-S) staining and immunostaining in wild type, APP/PS1 and APP/PS1 mice administrated by lactate. To validate lactate regulated by GPR81-PI3K/Akt/CREB -DNMT1 signaling pathway, we confirmed lactate and its regulation in cultured neurons using ELISA and immunostaining. It is observed that reduced lactate content is correlated with Aβ increase in cortex and hippocampus of APP/PS1 mice. Importantly, it signifies that reduced lactate and GPR81 lead to decrease of DNMT1. DNMT1 reduction promotes BACE1 expression, further increasing Aβ level. Otherwise, lactate administration reduces Aβ deposits in APP/PS1 mice. Besides, promotion of lactate content activates GPR81-PI3K/Akt/CREB signaling pathway. This work proves that lactate supplement reduces Aβ quantity, and underlying mechanism is that lactate activates GPR81-PI3K/Akt/CREB pathway which increases DNMT1, leading to the downregulation of BACE1 and Aβ levels.

Keywords: Lactate; Amyloid beta (Aβ); G protein-coupled receptor 81 (GPR81); Deoxyribonucleic acid methyltransferase 1 (DNMT1); Alzheimer's disease (AD)

Abbreviations

AD: Alzheimer Disease; ANOVA: One-Way Analysis of Variance; APP/PS1: Double-Transgenic Amyloid Precursor Protein/Presenilin 1; Aβ: Amyloid Beta; BACE1: Beta-Site Amyloid Precursor Protein Cleaving Enzyme 1; CREB: Cyclic-Adenosine-Monophosphate Response Element-Binding Protein; DAPI: 4,6-diamidino-2-phenylindole; 3,5 DHBA: 3,5-dihydroxybenzoic Acid; DNMT1: Deoxyribonucleic Acid Methyltransferase 1; ECL: Enhanced Chemiluminescence; ELISA: Enzyme Linked Immunosorbent Assay; ERK: Extracellular Regulated Protein Kinases; FITC: Isothiocyanate; GPR81: G Protein-Coupled Receptor 81; IPP: Image-Pro Plus; LDH: Lactate Dehydrogenase; LSD: Least Significant Difference; MCTs: Monocarboxylate Transporters; Neu N: Neuronal Nuclei; NFTs: Tau-Derived Neurofibrillary Tangles; NLRP3/NF-κB: Nod-like Receptor Family Pyrin Domain-Containing 3/Nuclear Factor-κB; OD: Optical Density; PBS: Phosphate Buffer Solution; PI3K/Akt: Phosphatidylinositol 3 Kinase /Protein Kinase B; PMSF: Phenylmethyl Sulfonylfluoride; PVDF: Polyvinylidenefluoride; RIPA: Radio-Immunoprecipitation Assay; SD: Standard Deviation; SDS-PAGE: Sodium Dodecyl Sulfate-Polyacrylamide Gel Electrophoresis; SPSS: Statistical Product and Service Solution; TBS: Tris-Buffered Saline; TBST: Tris-Buffered Saline Containing 0.1% Tween 20; Th-S: Thioflavin S; TRITC: Tetramethyl Rhodamine Isothiocyanate; WB: Western Bloting.

Introduction

Alzheimer disease (AD) is a neurodegenerative disorder characterized by progressive cognitive decline and dementia [1]. Genetic risk factors have been described in sporadic forms of AD. About 95% of AD is sporadic form, which is characterized by a late onset, and is the consequence of failure to clear amyloid beta (Aβ) peptide from the interstices of brain [2]. Continuous production of Aβ leads to aggregation of Aβ-containing amyloid plaques and accelerates tau-derived neurofibrillary tangles (NFTs), which ultimately leads to AD dementia [3]. Hence, cerebral accumulation of Aβ peptide is

Citation: Zhang M, Wang Y, Guan X, Chen X, Ge G, et al. Lactate May Reduce Aβ42 through Activating GPR81-PI3K/Akt/CREB-DNMT1 Signaling Pathway in APP/PS1 Mice. Austin J Clin Neurol. 2025; 12(1): 1171.

not merely an important molecular hallmark of AD [4], but it might become a promising target for AD prevention.

The decrease of Aβ aggregation can retard progressive axonal degeneration [5]. Unfortunately, two key questions remain unanswered: How to effectively lower Aβ production and promote Aβ clearance? Which stage of AD would be efficacy in an Aβ-directed preventive approach [6]? Previously, it is proved that Aβ clearance at early stage of AD mouse model, 3-month-old double-transgenic amyloid precursor protein/presenilin 1 (APP/PS1) mice, prevents Aβ plaque formation and benefits the delaying of AD onset [7]. Beta-site amyloid precursor protein cleaving enzyme 1 (BACE1) is an aspartic protease which functions in the first step of Aβ cleavage. Inhibition of BACE1 is being pursued to reduce amyloid deposition and accumulated Aβ plaques [8]. Meanwhile, deoxyribonucleic acid methyltransferase 1 (DNMT1) reduction leads to hypomethylation of specific loci within the BACE1 gene promoter. The lower expression of DNMT1, the higher level of BACE1 [9]. Hence, BACE1 expression might be negatively regulated by DNMT1.

On the other hand, Aβ increase is associated with inflammation, oxidative stress, and energy deficit [10]. glucose catabolism has been suppressed before Aβ deposits in the brains of familial AD individuals [11]. At this moment, lactate becomes the main energetic substrate of neurons, even it can defend against mitochondrial oxidation [12]. Also, the cultured neurons favoring glycolytic pathway resist against Aβ toxicity [13], and lactate administration can rescue the death of neurons [14]. Further, lactate is necessary for long-term memory formation and improvement of cognitive function [15]. Otherwise, there is a reduction of lactate level in the cortex and hippocampus of AD model mice [16,17]. But, the relation between cerebral lactate quantity and Aβ deposits in the brain of AD model mice hasn't been discussed.

Lactate transports from bloodstream across blood brain barrier via monocarboxylate transporters (MCTs) [18]. In the brain, lactate is temporarily stored in glial cells. During specific periods, such as brain development and AD, lactate can be quickly transported from glias to neurons and metabolized to sustain neuronal activity [19]. Therefore, lactate is normally recognized as a quickly energetic substrate of neurons. Actually, lactate is not merely an energy resource, but also plays as a signaling molecule [20]. G protein-coupled receptor 81 (GPR81) is a specific receptor of lactate. Its activation can trigger several signaling pathways, including phosphatidylinositol 3 kinase / protein kinase B (PI3K/Akt), extracellular regulated protein kinases (ERK1/2) pathway, Nod-like receptor family pyrin domain-containing 3/nuclear factor-κB (NLRP3/NF-κB) and so on [21]. Especially, it is recognized that the inhibition of PI3K/Akt pathway leads to DNMT1 downregulation [22]. Also, the dysregulation of PI3K/Akt signaling pathway results in tau hyperphosphorylation and Aβ deposition [23].

This work firstly discusses the relation between lactate content and Aβ deposits in APP/PS1 mice. It is evaluated the lactate content and GPR81 expression, and the downstream of GPR81, PI3K/Akt/cyclic-adenosine-monophosphate response element-binding protein (CREB) signaling pathway in wild type mice and APP/PS1 mice. Further, it is assessed expressions of DNMT1, BACE1 and Aβ42 in wild type mice and APP/PS1 mice. Then, correlation analysis was used to identify lactate content in relation with GPR81-PI3K/Akt-CREB signaling pathway, and levels of DNMT1, BACE1 and Aβ42 in wild type mice and APP/PS1 mice. Secondly, this study assesses the role of lactate administration in Aβ level in APP/PS1 mice and its underlying mechanism. Hence, lactate was given to APP/PS1 mice and also administrated to neurons to identify its regulative role in Aβ quantity, signaling pathway of GPR81-PI3K/Akt-CREB and DNMT1 expression.

Materials and Methods

Animals

3-month-old heterozygous APP/PS1 mice (n = 20) and their nontransgenic littermates (wild type, n = 10) were used in this study [24]. Animals were housed in individual cages in a controlled environment (temperature, 22 ± 1°C; humidity, 50% ± 10%; 12-hour light/12-hour dark cycle). Food and water were available ad libitum. Animals were grouped and named as Wild Type and APP/PS1. To assess the effect of lactate on Aβ deposits in AD model mice, 3-month-old APP/PS1 mice (n = 10) were administrated by intraperitoneal injection of lactate (117mg/kg). These mice were named as LAC group, and given thioflavin-S (Th-S) and immunofluorescence staining at the 6th month.

Primary Neuron Culture and Grouping

6-week-old C57BL/6 mice were obtained from the Experimental Animal Center of Army Medical University (Chongqing, China). The primary culture of cerebral cortical neurons from embryos of C57BL/6 mice was performed as previously described [25]. In brief, cerebral cortex of 18-day-old embryos was dissected from brain and then cut into slices. The slices were mechanically dissociated by trituration. The dissociated cells were suspended in Eagle's minimal essential medium supplemented with 3% B27 Minus AO, 10 μg/ml insulin, 0.25 μM glutamine, 1 mM β-hydroxybutyrate, 1 mM fumarate, and 50 ng/ml sodium selenite. Cell concentration was measured using a hemocytometer, and cells were plated at 6750 cells/mm^2 onto poly-D-lysine (Sigma)-coated 96-well and 6-well plates for immunostaining and western blotting (WB) analysis respectively. Cells were incubated at 37°C in a humidified atmosphere of 95 % O_2/5 % CO_2 for 14 days. To avoid glial cell growing and acquire purified neurons, cytosine arabinoside in a final concentration of 2.5ug/ml was added in the culture medium. Lactate in different concentrations (0 mM, 5 mM, 10 mM, 15 mM) and 10 mM lactate dehydrogenase (LDH) inhibitor (sodium oxamate) were administrated to neurons [26]. The groups were named as Control, 5mM LAC, 10mM LAC, 15mM LAC, and LAC Inhibitor.

Reagents and Antibodies

Radio-immunoprecipitation assay (RIPA) lysis buffer (Beyotime, Shanghai, China) and phenylmethyl sulfonylfluoride ([PMSF] Beyotime, Shanghai, China) were used to prepare homogenates of brain tissues. The BCA protein assay kit (Beyotime, Shanghai, China) was used to determine protein concentrations. Lactate levels were detected using a lactate assay kit (Nanjing Jiancheng, Jiangsu, China). Sodium dodecyl sulfate-polyacrylamide gel electrophoresis (SDS-PAGE), polyvinylidenefluoride (PVDF) filtermembranes (Bio-Rad, Hercules, CA), tris-buffered saline (TBS), tris-buffered saline containing 0.1% tween 20 ([TBST] Beyotime), and an enhanced

chemiluminescence (ECL) kit (Invitrogen, Carlsbad, CA) were used for WB analysis. ELISA MAX™ Deluxe Set Human Amyloid Beta (1-42) (Biolegend, California, America; #448704) was used to detect Aβ42 content in the brain. ELISA kits of p-PI3K, p-Akt and p-CREB (Saipeisheng, Shanghai, China; #SPS-13674, #SPS-13646, #SPS-13465) were used to assess p-PI3K, p-Akt and p-CREB contents of brain tissues.

Primary antibodies used in this study included mouse anti-beta actin ([anti-β-actin], Beyotime, Shanghai, China; #AF0003) [27], mouse anti-amyloid beta ([anti-Aβ] Covance, New Jersey, Princeton, USA; #803001) [7], mouse anti-neuronal nuclei ([anti-NeuN] Merck Millipore, Darmstadt, Germany; #MAB377X) [28], rabbit anti-GPR81 (Merck Millipore, Darmstadt, Germany; #SAB1301271) [29], rabbit anti-DNMT1 (Abcam, Cambridge, MA; # ab188453) [30], rabbit anti-BACE1 (Abcam, Cambridge, MA; #ab183612) [31], rabbit anti-phosphorylated PI3K (p-PI3K) p85/p55 (Cell Signaling Technology; Beverly, MA; #4228) [32], rabbit anti-PI3K (Cell Signaling Technology; Beverly, MA; #4257) [32], rabbit anti-phosphorylated Akt (p-Akt; Cell Signaling Technology; Beverly, MA; #4060) [32], rabbit anti-Akt (Cell Signaling Technology; Beverly, MA; #4691) [32], rabbit anti-phosphorylated CREB (p-CREB; Cell Signaling Technology; Beverly, MA; #9198) [32], rabbit anti-CREB (Cell Signaling Technology; Beverly, MA; #4820) [32]. Anti-mouse fluorescein isothiocyanate (FITC; Beyotime, Nanjing, China; #A0568) [33]and anti-rabbit tetramethyl rhodamine isothiocyanate (TRITC; Beyotime, Nanjing, China; #A0516) [33] secondary antibodies were used in immunofluorescence staining. 4,6-diamidino-2-phenylindole ([DAPI] Sigma, St. Louis, MO; #10236276001) [34] was applied to label nuclei. In addition, horseradish peroxidase conjugated secondary anti-mouse antibody (Beyotime, Shanghai, China; #A0239) [35] was used in WB. Primary antibodies used for immunostaining is in a dilution of 1:100, and primary antibodies used in WB is diluted in 1:1000. The specificity of the primary antibody has been checked in the reference of Bordeaux J and Uhlen M's studies [36,37].

Tissue Processing

Following perfusion with phosphate buffer solution (PBS), pH 7.4, the left hemispheres of brains from wild type and APP/PS1 groups (n = 5, respectively) were collected and stored in –20°C for lactate measurement. Meanwhile, the right hemispheres of brains were homogenized by RIPA lysis buffer containing 1mM PMSF. Brain tissues from cortex and hippocampus were homogenated, and centrifuged for 20 minutes at 14000 rpm. The obtained supernatant was assayed using the BCA protein assay kit and its concentration was adjusted to 1.5mg/mL. Finally, the samples were stored at –20°C for WB analysis. For immunohistochemical assay, wild type, APP/PS1 and LAC groups (n = 5, respectively) under anesthesia were perfused with saline followed by 4% paraformaldehyde in PBS and the brains were extracted and postfixed with fresh 4% paraformaldehyde at 4°C. Tissues were transferred to 30% sucrose solution for 2-3 days and subsequently cut into 20 μm slices.

Measurement of Lactate Concentration

Determinations of lactate concentration were performed with a lactate assay kit. The cortex and hippocampus were homogenized in saline at 4°C for 10 minutes, then the homogenates were centrifuged for 15 minutes at a speed of 2500 rpm. Assay buffers were added to the supernatants and incubated for 10 minutes at 37°C. Finally, optical density (OD) values were recorded at 530 nm after the reaction of lactate and assay buffers. Lactate content was calculated using the following formula:

Lactate content (mmol/g) = (OD measured value – OD blank value) / (OD standard value – OD blank value) × standard substance content (3 mmol/L) / protein content (g/L)

Quantitation of DNMT1 Gene Expression using RT-Qpcr

Total RNA was isolated from wild type and APP/PS1 groups using TriPure isolation reagent (Roche Applied Science, Germany) following the manufacturer's protocol. The quantity of extracted total RNA was determined spectrophotometrically using a Nanodropspectrophotometer (Thermo Fisher Scientific, USA). Total RNA integrity was evaluated using 2% formaldehyde containing 1.5 % agarose, and the purified RNA was stored at -80 °C until complementary DNA (cDNA) synthesis. The isolated RNA samples (1 μg) were treated with DNase I (Yekta Tajhiz Azma, Iran) to remove the genomic DNA. cDNA synthesis was performed using reverse transcriptase (RT) of 2 μg total RNA with oligo (dT) primers and M-MuLV RT (MBI Fermentas, Lithuania) in 20 μL reaction volumes. The mRNA expression levels of DNA methyltransferase 1 (DNMT1) were determined by RT-qPCR and SYBR Green qPCR Master Mix 2x (ABI, UK). RT-qPCR amplifications were performed in triplicate using a magnetic induction cycler (MIC) PCR system (Brisbane Queensland, Australia) under the following thermal cycling conditions: 95°C for 15 min, followed by 40 cycles of 95°C for 20 s, annealing at 60°C for 60 s, and a final extension at 72°C for 5 min. The primer sequence of DNMT1 is shown as follows. Gene Primer position: DNMT1 Primer (5' → 3'): Forward TACCTGGACGACCCTGACCT, Reverse CGTTGGCATCAAAGATGGACA; Product length: 103bp [38].

WB Analysis

Protein samples in the quantity of 30 μg were subjected to SDS-PAGE and transferred to PVDF filter membranes. The membranes were blocked with 5% nonfat milk for 1 hour at 37°C and incubated with primary antibodies for 12 hours at 4°C, including mouse anti-Aβ, mouse anti-p-PI3K, mouse anti-p85/p55, mouse anti-PI3Kp85, mouse anti-pAkt, mouse anti-Akt, mouse anti-pCREB, mouse anti-CREB. After washing with TBST, the membranes were incubated for secondary antibodies for 1 hour at 37°C and detected using ECL kit. Finally, the blots were qualified by Image J software (NIH, Bethesda, MD) [39], and the quantification of WB data was in the reference of Mahmood TSean C Taylor"s studies [40,41].

Immunofluorescence Staining

Brain sections were probed with mouse anti-Aβ, rabbit anti-GPR81, rabbit anti-DNMT1, rabbit anti-BACE1 primary antibodies, respectively. Brain sections were primarily blocked by 5% bovine serum albumin (BSA, Beyotime) for 30 minutes incubation at 37°C, and then incubated overnight with primary antibodies in a humidified chamber at 4°C. Sections were then washed 3 times with PBS for 5 minutes each, followed by incubation with anti-mouse FITC secondary antibody. For double-labeling immunofluorescence, sections were incubated with the mixture of 2 primary antibodies overnight at 4°C as

follows: Mouse anti-neuronal nuclei (Neu N) and rabbit anti-GPR81. Fluorescent secondary antibodies, raised in different species (FITC with green signal against mouse and TRITC with red signal against rabbit) were used to locate complexes of primary antibody. Cultured neurons from each group were prepared by five holes. Neurons were washed 3 times with PBS for 5 minutes, and incubated with rabbit anti-GPR81 and mouse anti-Neu N primary antibodies. Then, FITC with green signal against mouse and TRITC with red signal against rabbit were used to locate complexes of primary antibody. Nuclei were counterstained with DAPI for 5minutes. Moreover, negative control (no primary antibody) was used to check the specificity of secondary antibodies including FITC and TRITC.

Brain sections were observed under a fluorescence microscope (Olympus, Tokyo, Japan), which covers a total area of 0.19 mm^2. Five different fields (0.50 to 0.38 mm in the penumbra of the brain tissues) per mouse, and five mice per group were assessed. FITC, TRITC and DAPI filters were chosen to capture the images. Images were obtained at 200× magnification. Immunoreactive cells were obtained at 400× magnification. Positive expressions of staining pictures were analyzed by the values of OD. OD values were calculated using Image-Pro Plus 6.0 (IPP6.0) software according to manufacturer's instructions [42].

Thioflavin S (Th-S) Staining

Brain sections were washed with distilled water and stained in a 1% Th-S staining solution for 5 min. 70% ethanol was used to differentiate sections for 1 min and mounted in 50% glycerin. Fluorescence microscope (Olympus, Tokyo, Japan) was used to detect positive Th-S staining. Aβ plaques were determined separately in the cortex and hippocampus. Th-S staining area was carried out under × 200 microscopic magnification and was counted on every five fields throughout the entire cortex and hippocampus by the Image-Pro Plus 6.0 software. Positive Aβ staining area (%) was calculated relative to the total area of the analyzed region (area% = plaque area/ total area selected × 100%).

Statistical Analysis

Five APP/PS1 mice and five wild type mice were used for immunohistochemical assay and WB analysis respectively (n = 5). Five holes have been prepared in each group of neurons (n = 5) [43]. G*power method was used to calculate the sample size. Further, in order to determine the effect size, f = 0.6 with a power of 83% in a one-way between-subjects ANOVA (two groups/five groups, alpha=0.05), G*Power suggested 5 samples in each group. Data were analyzed using GraphPad Prism 9 (GraphPad Software, La Jolla, CA, USA). Variance was evaluated with the Brown-Forsythe test and then the normal distribution of the data was evaluated by Shapiro. To confirm that the data have a normal distribution, statistical evaluation by one-way ANOVA, followed by Tukey Post hoc test was conformed. The results of all experiments were averaged three times and performed mean ± Standard Deviation (SD) independently. Pearson method was applied to determine the correlation between lactate and p-PI3K/PI3K, p-Akt/Akt or p-CREB/CREB, between p-CREB/CREB and DNMT1 or BACE1, between DNMT1 and BACE1 or Aβ. Data were analyzed with one-way ANOVA to calculate the significance level. Differences with $^*P < 0.05$ and $^{**}P < 0.01$ were considered statistically significant. All statistical analyses were done in a blind manner, in which another experimenter who does not know the identity of the data independently analyzes the data [44,45].

Results

Lactate and its Downstream GPR81-PI3K/Akt-CREB are Suppressed in the Cortex and Hippocampus of APP/PS1 Mice

Lactate contents in the cortex and hippocampus of APP/PS1 mice are 5.1 ± 1.28 mmol/g and 5.29 ± 1.76 mmol/g, which are lower than those of wild type mice in the cortex (14.8 ± 1.13 mmol/g) and hippocampus (15.91 ± 1.03 mmol/g) ($^*P < 0.05$, Figure 1A). As arrowheads pointed, positive staining of GPR81 can be found in the cortex and hippocampus of APP/PS1 mice and wild type mice (Figure 1B). In statistic, OD values of GPR81 in cortex and hippocampus of APP/PS1 are 21196 ± 2187 and 18503 ± 1895, which are lower than those of wild type mice (32741 ± 3012 in cortex and 27332.3 ± 2198 in hippocampus) ($^*P < 0.05$, Figure 1C).

Expressions of p-PI3K, p-Akt, p-CREB were assessed by WB (Figure 1D). Statistically, relative levels of p-PI3K, p-Akt and p-CREB in wild type mice are 0.43 ± 0.04, 0.38 ± 0.03, 0.97 ± 0.02, which are lower than those of APP/PS1 mice (0.17 ± 0.02, 0.18 ± 0.01, 0.59 ± 0.01 respectively) ($^*P < 0.05$, Figure 1E).

There is a Reduction of DNMT1, Increase of BACE1 and Aβ in the Cortex and Hippocampus of APP/PS1 Mice

The mRNA level of DNMT1 was determined in brain tissues of APP/PS1 mice and wild type mice using RT-qPCR. The results showed

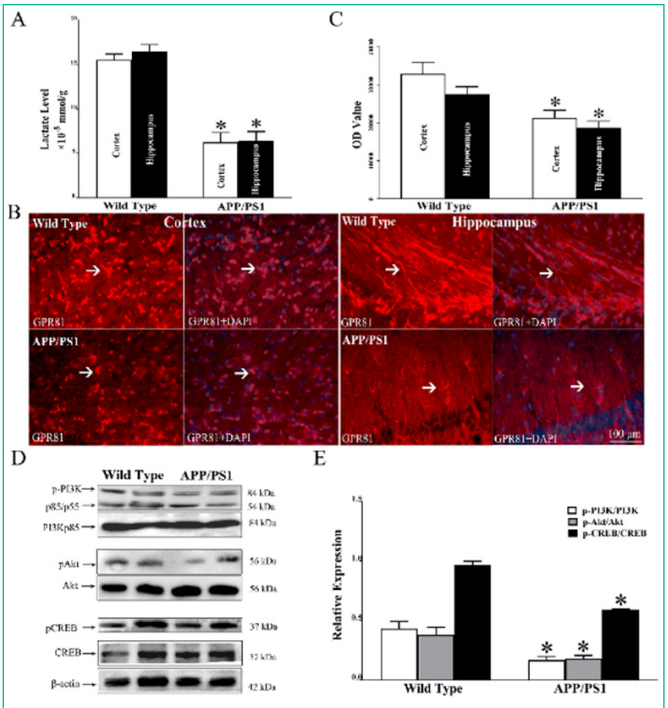

Figure 1: In comparison with wild type mice, lactate and GPR81-PI3K/Akt-CREB signaling pathway are suppressed in the cortex and hippocampus of APP/PS1 mice. (A) Lactate quantity is decreased in the cortex and hippocampus of APP/PS1 mice compared with wild type mice. (B) Positive expression of GPR81 can be found in the cortex and hippocampus of APP/PS1 mice and wild type mice. (C) In comparison with wild type mice, relative expression of GPR81 is reduced in the cortex and hippocampus of APP/PS1 mice. (D) WB was used to assess expressions of p-PI3K, p-Akt, p-CREB. (E) Compared with wild type mice, relative levels of p-PI3K, p-Akt and p-CREB in APP/PS1 mice are reduced. (N = 5 mice per group. $^*P < 0.05$).

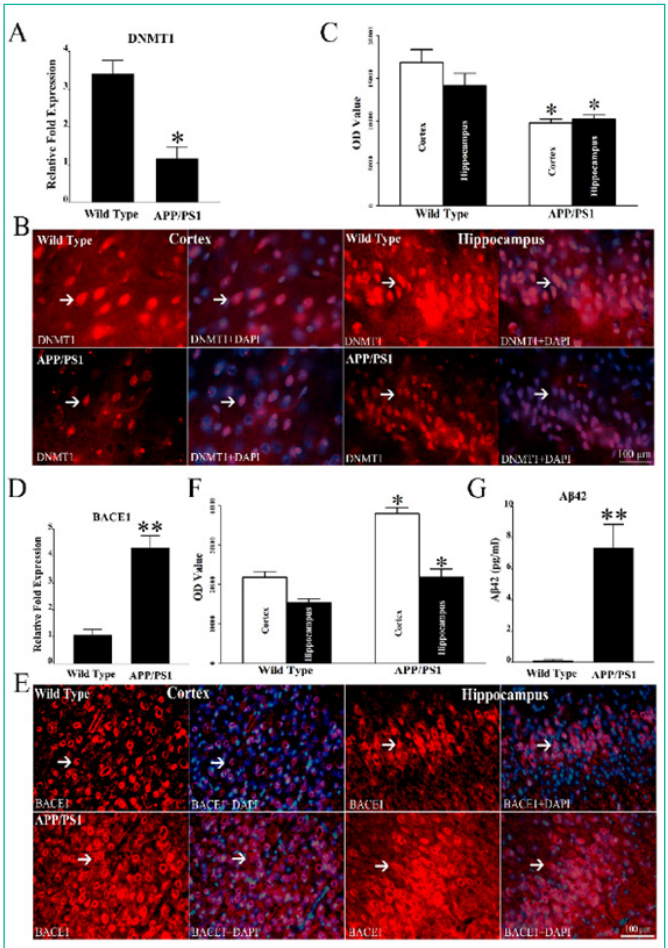

Figure 2: Compared with wild type mice, there is a reduction of DNMT1, increase of BACE1 expression and Aβ level in the cortex and hippocampus of APP/PS1 mice. (A) Through RT-qPCR analysis, it is found that mRNA expression of DNMT1 is reduced in the cortex and hippocampus of APP/PS1 mice in comparison with wild type mice. (B) Through immunostaining, DNMT1, mainly localized in the nuclei, can be found in the cortex and hippocampus of APP/PS1 mice and wild type mice. (C) There is a reduction of DNMT1 in the cortex and hippocampus of APP/PS1 mice in comparison with wild type mice. (D) RT-qPCR was used to evaluate mRNA level of BACE1, and there is a striking increase of BACE1 mRNA level in APP/PS1 mice compared with wild type mice. (E) Positive expression of BACE1 can be found in the cortex and hippocampus of APP/PS1 mice and wild type mice. (F) In comparison with wild type mice, OD values of BACE1 expressions are upregulated in the cortex and hippocampus of APP/PS1 mice. (G) ELISA was used to evaluate Aβ42 level, and Aβ42 level of brain tissue in APP/PS1 mice is strikingly higher than that of wild type mice. (N = 5 mice per group. $^{*}P < 0.05$, $^{**}P < 0.01$).

that mRNA expression of DNMT1 is reduced in APP/PS1 mice compared to wild type mice ($^{*}P < 0.05$, Figure 2A). Immunostaining was used to assess DNMT1 expression in the cortex and hippocampus of APP/PS1 mice and wild type mice. DNMT1 locates in the nucleus in the cortex and hippocampus of APP/PS1 mice and wild type mice (Figure 2B). In statistic, OD values of DNMT1 in cortex and hippocampus of wild type mice are 16863 ± 1486 and 14157 ± 1521. Otherwise, in the cortex and hippocampus of APP/PS1 mice, OD values are 10057 ± 428 and 9900 ± 568, which are lower than those of wild type mice ($^{*}P < 0.05$, Figure 2C). In APP/PS1 mice and wild type mice, mRNA level of BACE1 was evaluated using RT-qPCR, and the results showed that mRNA level of BACE1 is strikingly elevated in APP/PS1 mice in comparison with wild type mice ($^{**}P < 0.01$, Figure 2D). BACE1 is positively labeled in the cortex and hippocampus of APP/PS1 mice and wild type mice (Figure 2E). In the cortex and hippocampus of APP/PS1 mice, OD values of BACE1 are 38036 ± 1299 and 21917 ± 2229, which are higher than those of wild type mice, 21896 ± 1595 in cortex and 15333 ± 1052 in hippocampus ($^{*}P < 0.05$, Figure 2F). Aβ42 level was determined by ELISA, and the results showed that Aβ42 level of brain tissue in APP/PS1 mice is strikingly higher than that of wild type mice ($^{**}P < 0.01$, Figure 2G).

Lactate is Positively Correlated with GPR81-PI3K/Akt/CREB-DNMT1 Signaling Pathway, while it is in a Negative Correlation with the Levels of BACE1 and Aβ42 in APP/PS1 Mice

Through correlative analysis, lactate content is positively

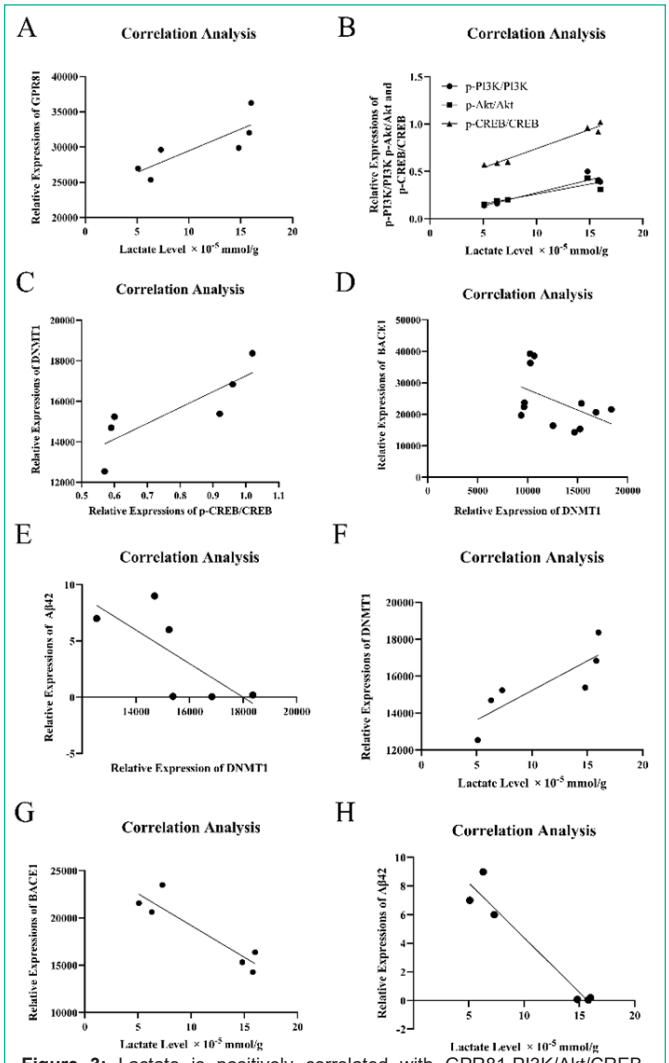

Figure 3: Lactate is positively correlated with GPR81-PI3K/Akt/CREB-DNMT1 signaling pathway, but negatively correlated with the level of BACE1 and Aβ42. (A) Correlative analysis reveals a positive correlation between lactate content and GPR81 expression. (B) lactate quantity is positively correlated with p-PI3K, p-AKT and p-CREB. (C) There is a positive correlation between p-CREB and DNMT1. (D) DNMT1 is negatively correlative with BACE1. (E) DNMT1 is in a negative correlation with Aβ42. (F) Lactate level is positive correlated with DNMT1. (G) Lactate quantity is in a negative correlation with BACE1. (H) Lactate content is negatively correlated with Aβ42. (N = 6-12 mice per group. $^{*}P < 0.05$).

correlated with expressions of GPR81, p-PI3K, p-AKT and p-CREB. Specifically, the relevant formulas of lactate and GPR81, lactate and p-PI3K, lactate and p-AKT, lactate and p-CREB are $Y = 614.5*X + 23349$, $Y = 0.02753*X - 0.001257$, $0.02092*X + 0.05233$ and $Y = 0.04024*X + 0.3387$ ($*P < 0.05$, Figure 3A and 3B). Importantly, p-CREB is positively correlative with DNMT1, while DNMT1 is negatively correlative with BACE1 and Aβ42. The formulas are $Y = 7812*X + 9443$, $Y = -1.299*X + 40848$, $Y = -0.001493*X + 26.88$ respectively ($*P < 0.05$, Figure 3C, 3D and 3E). Further, correlation between lactate content and DNMT1 (BACE1, Aβ42) was assessed. It shows that lactate level is positively related with DNMT1, while negatively correlated with BACE1 and Aβ42. The formulas are $Y = 320.0*X + 12027$, $Y = -671.8*X + 25926$, $Y = -0.7644*X + 12.04$ ($*P < 0.05$, Figure 3F, 3G and 3H).

Lactate Suppresses Aβ Deposits in the Cortex and Hippocampus of APP/PS1 Mice

Through correlative analysis, it shows that lactate is in a negative correlation with Aβ42. Here, it is further assessed the effect of lactate administration on Aβ deposits in APP/PS1 mice through Th-S staining and immunostaining. Th-S staining was used to evaluate Aβ deposits in the cortex and hippocampus of wild type mice, APP/PS1 mice and APP/PS1 mice administrated by lactate (LAC group). Aβ deposits (green) are distributed throughout the cortex and hippocampus in the APP/PS1 group compared to wild type group and LAC group (Figure 4A). In statistic, the areas of Aβ Th-S staining in cortex of wild type, APP/PS1 and LAC groups are 0.021 ± 0.001, 1.433 ± 0.003 and 0.143 ± 0.002. The areas of Aβ Th-S staining in hippocampus of wild type, APP/PS1 and LAC groups are 0.017 ± 0.001, 2.033 ± 0.004 and 0.46 ± 0.002. Positive Th-S staining of Aβ deposits in APP/PS1 group is higher than that of wild type and LAC groups ($**P < 0.01$, $*P < 0.05$, Figure 4B). Immunostaining was used evaluate insoluble Aβ42 in the cortex and hippocampus of wild type, APP/PS1 and LAC groups. The results show that insoluble Aβ42 (red) spreads in the cortex and hippocampus of APP/PS1 group, but not in wild type and LAC groups (Figure 4C). OD values of insoluble Aβ42 in the cortex of wild type, APP/PS1 and LAC groups are 106 ± 9, 9592 ± 38 and 194 ± 8. In the hippocampus, OD values of insoluble Aβ42 in wild type, APP/PS1 and LAC groups are 126 ± 8, 11500 ± 32 and 216 ± 6 ($**P < 0.01$, Figure 4D).

Lactate Activates GPR81-PI3K/Akt/CREB-DNMT1 Signaling Pathway in Cultured Neurons

Cultured neurons were divided into 5 groups and given different administrations. Neurons from 5 groups were given 0 mM, 5 mM, 10 mM, 15 mM lactate and 10 mM LDH inhibitor (sodium oxamate) for 24 hours, and named as Control, 5mM LAC, 10mM LAC, 15mM LAC, and Inhibitor. Besides, 10 mM LDH inhibitor (sodium oxamate) was given to reduce lactate level in cultured neurons. Then, expressions of GPR81, p-PI3K, p-Akt, p-CREB and DNMT1 were assessed to identify the effect of lactate addition and lactate removal on GPR81-PI3K/Akt/CREB-DNMT1 signaling pathway.

The cells were double stained by GPR81 (red) and Neu N (green) (Figure 5A). In statistic, OD values of GPR81 (red) are 46525 ± 1983, 55061 ± 1823, 61165 ± 2330, 52608 ± 1390 and 36800 ± 1711 in Control, 5 mM, 10 mM, 15mM and Inhibitor groups respectively. OD values of Neu N (green) are 35717 ± 3019, 35334 ± 1558, 33931 ± 1758, 34275 ± 1693 and 35161 ± 593 in each group. There is an increase of GPR81 expression in 10 mM group, and a reduction in GPR81 expression in the group of LDH Inhibitor compared with Control group ($*P < 0.05$, Figure 5B). No differences of Neu N expressions can be found in each group ($P > 0.05$, Figure 5B). ELISA was used to

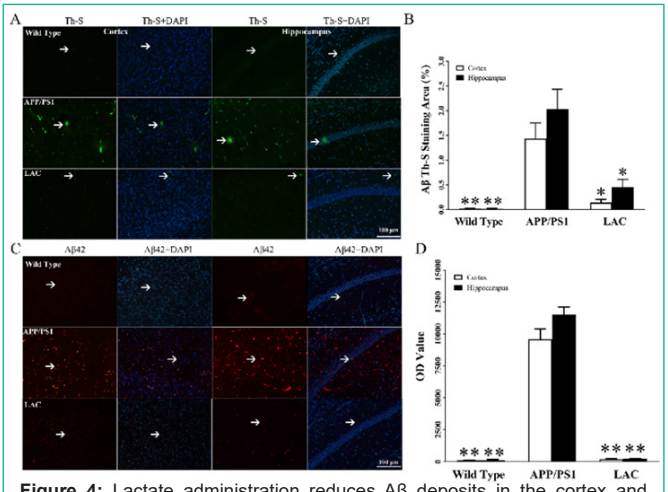

Figure 4: Lactate administration reduces Aβ deposits in the cortex and hippocampus of APP/PS1 mice. (A) Through Th-S staining, it is observed Aβ deposits in the cortex and hippocampus of APP/PS1 group. (B) Compared with wild type group, Aβ deposits are obviously increased in the cortex and hippocampus of APP/PS1 group. There is a decrease of Aβ deposits in the cortex and hippocampus of LAC group compared with APP/PS1 group. (C) As arrowheads pointed, Aβ42 can be found in the cortex and hippocampus of APP/PS1 and LAC groups. (D) OD values of Aβ42 in the cortex and hippocampus of APP/PS1 group are higher than those of wild type group. OD values of Aβ42 in the cortex and hippocampus of LAC group are reduced in comparison with APP/PS1 group. (N = 5 mice per group. $*P < 0.05$, $**P < 0.01$).

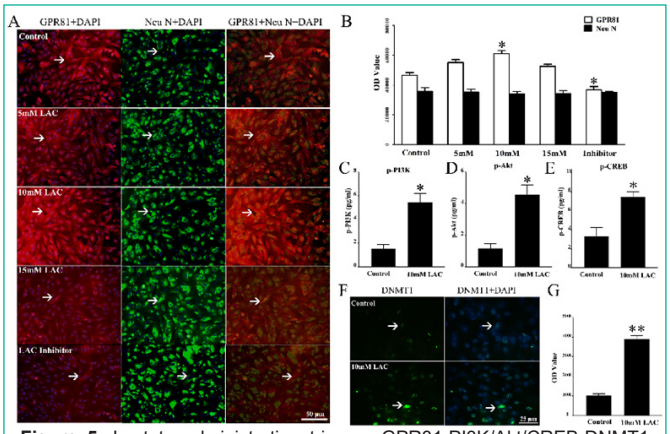

Figure 5: Lactate administration triggers GPR81-PI3K/Akt/CREB-DNMT1 signaling pathway in cultured neurons. (A) Through double staining of GPR81 (red) and Neu N (green), GPR81 expression is recognized at cell surface of neurons. (B) In comparison with Control group, 10 mM lactate increases GPR81 expression in cultured neurons. Otherwise, 10 mM LDH inhibitor leads to lactate deficit, which downregulates GPR81 expression in cultured neurons. (C) Through ELISA analysis, it is recognized that p-PI3K level in 10mM LAC group is higher than that of Control group. (D) There is an increase of p-Akt content in 10mM LAC group compared with Control group. (E) p-CREB quantity in 10mM LAC group is increased compared with Control group. (F) DNMT1 expression (green) in Control and 10mM LAC group was assessed by immunostaining. (G) DNMT1 expression in 10 mM LAC group is obviously higher than that of Control group. (N = 5 mice per group. $*P < 0.05$, $**P < 0.01$).

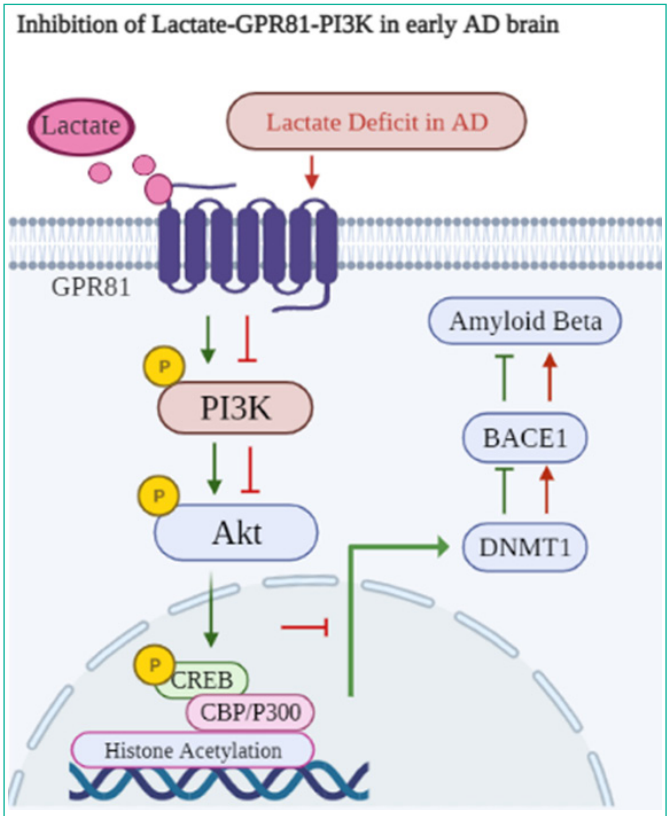

Figure 6: In physiological condition, lactate binds to its receptor GPR81, and then activates PI3K/Akt/CREB signaling pathway. Moreover, activation of this pathway promotes histone acetylaiton of DNMT1 gene. Further, DNMT1 expression is increased, and DNMT1 is significant for methylation of specific loci within the BACE1 gene promoter. Therefore, DNMT1 expression can suppress BACE1 level and Aβ production. Otherwise, lactate reduction in AD model mice results in the suppression of GPR81-PI3K/Akt/CREB signaling pathway, which downregulates DNMT1 expression. As a result, BACE1 level is increased, contributing to the upregulation Aβ level.GPR81 (red) and Neu N (green), GPR81 expression is recognized at cell surface of neurons. (B) In comparison with Control group, 10 mM lactate increases GPR81 expression in cultured neurons. Otherwise, 10 mM LDH inhibitor leads to lactate deficit, which downregulates GPR81 expression in cultured neurons. (C) Through ELISA analysis, it is recognized that p-PI3K level in 10mM LAC group is higher than that of Control group. (D) There is an increase of p-Akt content in 10mM LAC group compared with Control group. (E) p-CREB quantity in 10mM LAC group is increased compared with Control group. (F) DNMT1 expression (green) in Control and 10mM LAC group was assessed by immunostaining. (G) DNMT1 expression in 10 mM LAC group is obviously higher than that of Control group. (N = 5 mice per group. $*P < 0.05$, $**P < 0.01$).

detect expressions of p-PI3K, p-Akt, p-CREB in Control and 10mM LAC groups. Levels of p-PI3K, p-Akt, p-CREB in 10mM LAC group are increased compared with Control group ($*P < 0.05$, Figure 5C, 5D and 5E). Immunostaining was used to detect DNMT1 expression in Control and 10mM LAC groups, and DNMT1 (green) locates in cell nucleus (Figure 5F). There is an obvious increase of DNMT1 in cultured neurons after 10 mM lactate administration ($**P < 0.01$, Figure 5G). These results reveal that lactate can effectively activate neuronal GPR81-PI3K/Akt/CREB signaling pathway and upregulate DNMT1 expression *in vitro*.

Discussion and Conclusion

During AD progression, Aβ deposition starts with the production of insoluble Aβ fibrils. Hence, downregulation of Aβ in AD brain might be a promising therapeutic strategy [46]. BACE1 is the rate-limiting enzyme of insoluble Aβ cleavage, which cleaves amyloid precursor protein to produce insoluble Aβ [46]. Meanwhile, promoter of BACE1 gene in AD subjects is hypomethylation, which is related with the reduction of DNMT1 [47,48]. Moreover, inhibition of PI3K/Akt signaling pathway aggravates Aβ accumulation [49]. Especially, PI3K/Akt pathway can be activated by lactate and its receptor GPR81 [22]. Previously, lactate is normally considered as an unwanted or toxic metabolite in 1930s [50]. Until 1950s, lactate is recognized as an alternative energy substrate [51]. Even, recent studies signify that lactate is not merely an energy substrate of neurons, but also plays as a signaling molecule, regulating neuronal activity [52].

In this work, it discusses the relation between lactate and Aβ level in AD brain. It is recognized that lactate content, GPR81 expression and phosphorylation of PI3K/Akt/CREB are reduced in APP/PS1 mice compared with wild type mice. Further, it is observed a decrease of DNMT1, an increase of BACE1 and Aβ in the cortex and hippocampus of APP/PS1 mice.

Significantly, correlative analysis reveals that lactate positively correlates with GPR81-PI3K/Akt/CREB pathway and DNMT1 expression, but negatively correlates with expressions of BACE1 and Aβ42 in APP/PS1 mice. Then, lactate was administrated to APP/PS1 mice, which effectively decreases Aβ deposits in the cortex and hippocampus of APP/PS1 mice. Further, it is observed that lactate directly activates GPR81-PI3K/Akt/CREB signaling pathway in cultured neurons.

Conclusively, this study reveals that lactate reduction is correlated with increased Aβ level in AD model mice. As results showed, lactate level, phosphorylation of GPR81-PI3K/Akt/CREB and DNMT1 expression are reduced, expressions of BACE1 and Aβ are increased in the cortex and hippocampus of APP/PS1 mice. Through correlation analysis, it is found that lactate is positively related with GPR81 downstream and DNMT1, and negatively associated with BACE1 and Aβ. Meanwhile, the increase of lactate content downregulates Aβ deposits in the cortex and hippocampus of APP/PS1 mice, which also activates GPR81-PI3K/Akt/CREB pathway and promotes DNMT1 expression in culture neurons. Therefore, it is proved that lactate activates GPR81 and its downstream of PI3K/Akt/CREB-DNMT1 signaling pathway, resulting in reduction of BACE1 and Aβ. But, the downregulation of lactate may inhibit GPR81-PI3K/Akt/CREB-DNMT1 signaling pathway and increase BACE1 and Aβ expressions in APP/PS1 mice (Figure 6).

Availability of Data and Materials

The datasets used and/or analyzed during the current study are available from the corresponding author on reasonable request.

Author Contributions

Mao Zhang and Hong Guo contributed to the conception of this study. Data acquisition was performed by Mao Zhang, Yanyan Wang, Xingying Guan, Xuedan Chen and Guodong Ge. Data analysis was performed by Mao Zhang. The interpretation of the data was done by Mao Zhang. The funding acquisition was granted by Mao Zhang. The first draft of the manuscript was written by Mao Zhang. The final version of this article was revised by Hong Guo.

Ethics Approval and Consent to Publication

All procedures were carried out in accordance with the National Institute of Health Guide for the Care and Use of Laboratory Animals (NIH Publications No. 80-23, revised 1996). All experiments in this study were performed in accordance with protocols specifically approved (IACUC: 09446) by the Army Medical University Institutional Animal Care and Use Committee.

Funding

This work was supported by grants from Natural Science Foundation of Chongqing (Grant No. CSTB2024NSCQ-MSX0558) and Science and Technology Research Project of Chongqing Education Commission (Grant No. KJQN202412808).

References

1. Armstrong R. Risk factors for Alzheimer's disease. Folia Neuropathol. 2019; 57: 87-105.
2. Lili Zhang, Chen Chen, Marvin Sh Mak, Junfeng Lu, Zeqing Wu, Qiuhe Chen, et al. Advance of sporadic Alzheimer's disease animal models. Med Res Rev. 2020; 40: 431-458.
3. Tiwari S, Atluri V, Kaushik A, Yndart A, Nair M. Alzheimer's disease: pathogenesis, diagnostics, and therapeutics. Int J Nanomedicine. 2019; 14: 5541-5554.
4. De Strooper B, Karran E. The cellular phase of Alzheimer's disease. Cell. 2016; 164: 603-615.
5. Natalia Salvadores, Cristian Gerónimo Olvera, Felipe A Court. Axonal degeneration in AD: The contribution of Aβ and Tau. Front Aging Neurosci. 2020; 12: 581767.
6. Loeffler DA. Antibody-mediated clearance of brain amyloid-β: Mechanisms of action, effects of natural and monoclonal anti-Aβ antibodies, and downstream effects. J Alzheimers Dis Rep. 2023; 7: 873-899.
7. Weixi Feng, Yanli Zhang, Ze Wang, Hanrong Xu, Ting Wu, Charles Marshall, et al. Microglia prevent beta-amyloid plaque formation in the early stage of an Alzheimer's disease mouse model with suppression of glymphatic clearance. Alzheimers Res Ther. 2020; 12: 125.
8. Neeraj Singh, Brati Das, John Zhou, Xiangyou Hu, Riqiang Yan. Targeted BACE-1 inhibition in microglia enhances amyloid clearance and improved cognitive performance. Sci Adv. 2022; 8: eabo3610.
9. Huang P, Sun J, Wang F, Luo X, Zhu H, Gu Q, et al. DNMT1 and Sp1 competitively regulate the expression of BACE1 in A2E-mediated photo-oxidative damage in RPE cells. Neurochem Int. 2018; 121: 59-68.
10. Ashu Johri. Disentangling mitochondria in Alzheimer's disease. Int J Mol Sci. 2021; 22: 11520.
11. Qianqian Wang, Linyan Duan, Xingfan Li, Yifu Wang, Wenna Guo, Fangxia Guan, et al. Glucose metabolism, neural cell senescence and Alzheimer's disease. Int J Mol Sci. 2022; 23: 4351.
12. Richard A Harris, Lauren Tindale, Asad Lone, Olivia Singh, Shannon L Macauley, Molly Stanley, et al. Aerobic glycolysis in the frontal cortex correlates with memory performance in wild-type mice but not the APP/PS1 mouse model of cerebral amyloidosis. J Neurosci. 2016; 36: 1871-1878.
13. Jordan T Newington, Andrea Pitts, Andrew Chien, Robert Arseneault, David Schubert, Robert C Cumming. Amyloid beta resistance in nerve cell lines is mediated by the Warburg effect. PLoS One. 2011; 6: e19191.
14. Won SJ, Jang BG, Yoo BH, Sohn M, Lee MW, Choi BY, et al. Prevention of acute/severe hypoglycemia-induced neuron death by lactate administration. J Cereb Blood Flow Metab. 2012; 32: 1086-1096.
15. El Hayek L, Khalifeh M, Zibara V, Abi Assaad R, Emmanuel N, Karnib N, et al. Lactate mediates the effects of exercise on learning and memory through SIRT1-dependent activation of hippocampal brain-derived neurotrophic factor (BDNF). J Neurosci. 2019; 39: 2369-2382.
16. Mao Zhang, Xiaofang Cheng, Ruozhi Dang, Weiwei Zhang, Jie Zhang, Zhongxiang Yao. Lactate deficit in an Alzheimer disease mouse model: The relationship with neuronal damage. J Neuropathol Exp Neurol. 2018; 77: 1163-1176.
17. Liguori C, Chiaravalloti A, Sancesario G, Stefani A, Sancesario GM, Mercuri NB, et al. Cerebrospinal fluid lactate levels and brain [18F]FDG PET hypometabolism within the default mode network in Alzheimer's disease. Eur J Nucl Med Mol Imaging. 2016; 43: 2040-2049.
18. Melanie A Felmlee, Robert S Jones, Vivian Rodriguez Cruz, Kristin E Follman, Marilyn E Morris. Monocarboxylate transporters (SLC16): function, regulation, and role in health and disease. Pharmacol Rev. 2020; 72: 466-485.
19. Firth J, Stubbs B, Vancampfort D, Schuch F, Lagopoulos J, Rosenbaum S, Ward PB. Effect of aerobic exercise on hippocampal volume in humans: a systematic review and meta-analysis. Neuroimage. 2018; 166: 230-238.
20. Bergersen LH. Lactate transport and signaling in the brain: Potential therapeutic targets and roles in body-brain interaction. Journal of Cerebral Blood Flow & Metabolism. 2015; 35: 176-185.
21. Jingyun Hu, Ming Cai, Yuran Liu, Beibei Liu, Xiangli Xue, Ruifang Ji, et al. The roles of GRP81 as a metabolic sensor and inflammatory mediator. J Cell Physiol. 2020; 235: 8938-8950.
22. Ying Zhang, Nan Qu Huang, Fei Yan, Hai Jin, ShaoYu, Zhou Jing, et al. Diabetes mellitus and Alzheimer's disease: GSK-3β as a potential link Affiliations expand. Behav Brain Res. 2018; 339: 57-65.
23. Rongfeng Xu, Yuning Sun, Zhongpu Chen, Yuyu Yao, Genshan Ma. Hypoxic preconditioning inhibits hypoxia-induced apoptosis of cardiac progenitor cells via the PI3K/Akt-DNMT1-p53 Pathway. Sci Rep. 2016; 6: 30922.
24. JJ Gallagher, A M Minogue, MA Lynch. Impaired performance of female APP/PS1 mice in the Morris water maze is coupled with increased Aβ accumulation and microglial activation. Neurodegener Dis. 2013; 11: 33-41.
25. Hong Zhao, ZhiHong Ji, Chao Liu, XinYu Yu. Neuroprotective mechanisms of 9-Hydroxy epinootkatol against glutamate-induced neuronal apoptosis in primary neuron culture. J Mol Neurosci. 2015; 56: 808-814.
26. Young A, Oldford C, Mailloux RJ. Lactate dehydrogenase supports lactate oxidation in mitochondria isolated from different mouse tissues. Redox Biol. 2020; 28: 101339.
27. Wenjin Guo, Shuai Lian, Li Zhen, Shucheng Zang, Yan Chen, Limin Lang, et al. The favored mechanism for coping with acute cold stress: Upregulation of miR-210 in rats. Cell Physiol Biochem. 2018; 46: 2090-2102.
28. Anna Piotrowska, Ewelina Rojewska, Katarzyna Pawlik, Grzegorz Kreiner, Agata Ciechanowska, Wioletta Makuch, et al. Pharmacological blockade of spinal CXCL3/CXCR2 signaling by NVP CXCR2 20, a selective CXCR2 sntagonist, reduces neuropathic pain following peripheral nerve injury. Front Immunol. 2019; 10: 2198.
29. Rupali Vohra, Blanca I Aldana, Helle Waagepetersen, Linda H Bergersen, Miriam Kolko. Dual properties of lactate in müller cells: The effect of GPR81 activation. Invest Ophthalmol Vis Sci. 2019; 60: 999-1008.
30. Yan Lu, Huinan Qu, Da Qi, Wenhong Xu, Shutong Liu, Xiangshu Jin, Peiye Song, Yantong Guo, et al. OCT4 maintains self-renewal and reverses senescence in human hair follicle mesenchymal stem cells through the downregulation of p21 by DNA methyltransferases. Stem Cell Research & Therapy. 2019; 10: 28.
31. Marlen Dierich, Stephanie Hartmann, Nadine Dietrich, Philip Moeser, Franziska Brede, Lejo Johnson Chacko, et al. β-Secretase BACE1 Is Required for Normal Cochlear Function. J Neurosci. 2019; 39: 9013-9027.
32. Shenshen Zhang, Ran Xue, Yaping Geng, Hao Wang, Wenjie Li. Fisetin prevents HT22 cells from high glucose-induced neurotoxicity via PI3K/Akt/CREB signaling pathway. Front Neurosci. 2020; 14: 241.
33. Yanying Zhao, Junni Tang, Danru Yang, Cheng Tang, Juan Chen. Staphylococcal enterotoxin M induced inflammation and impairment of bovine mammary epithelial cells. J Dairy Sci. 2020;103: 8350-8359.
34. Omman R, Kwong C, Shepherd D, Molnar JA, Velankar MM, Mirza KM. Revisiting howell-jolly body-like cytoplasmic inclusions in neutrophils: A report of two cases and confirmation of nuclear origin. J Hematol. 2017; 6: 101-104.

35. Zhang Q, He D, Xu L, Ge S, Wang J, Zhang X. Generation and evaluation of anti-mouse IgG IgY as secondary antibody. Prep Biochem Biotechnol. 2020; 50: 788-793.

36. Bordeaux J, Welsh A, Agarwal S, Killiam E, Baquero M, Hanna J, et al. Antibody validation. Biotechniques. 2010; 48: 197-209.

37. Mathias Uhlen, Anita Bandrowski, Steven Carr, Aled Edwards, Jan Ellenberg, Emma Lundberg, et al. A proposal for validation of antibodies. Nat Methods. 2016; 13: 823-827.

38. Mona Moghadasi, Mozhgan Taherimoghaddam, Esmaeel Babaeenezhad, Mehdi Birjandi, Mozhgan Kaviani, Mostafa Moradi Sarabi. MicroRNA-34a and promoter methylation contribute to peroxisome proliferator-activated receptor gamma gene expression in patients with type 2 diabetes. Diabetes Metab Syndr. 2024; 18: 103156.

39. Sarawut Lapmanee, Jantarima Charoenphandhu, Jarinthorn Teerapornpuntakit, Nateetip Krishnamra, Narattaphol Charoenphandhu. Agomelatine, venlafaxine, and running exercise effectively prevent anxiety- and depression-like behaviors and memory impairment in restraint stressed rats. PLoS One. 2017; 12: e0187671.

40. Mahmood T, Yang PC. Western blot: technique, theory, and trouble shooting. N Am J Med Sci. 2012; 4: 429-434.

41. Sean C Taylor, Thomas Berkelman, Geetha Yadav, Matt Hammond. A defined methodology for reliable quantification of Western blot data. Mol Biotechnol. 2013; 55: 217-226.

42. Zhang Y, Lan F, Li Y, Wang C, Zhang L. Formation of papillary mucosa folds and enhancement of epithelial barrier in odontogenic sinusitis. Int Forum Allergy Rhinol. 2019; 9: 1281-1288.

43. Kadam P, Bhalerao S. Sample size calculation. Int J Ayurveda Res. 2010; 1: 55-57.

44. Michel MC, Murphy TJ, Motulsky HJ. New author guidelines for displaying data and reporting data analysis and statistical methods in Experimental Biology. J Pharmacol Exp Ther. 2020; 372: 136-147.

45. Weissgerber TL, Milic NM, Winham SJ, Garovic VD. Beyond bar and line graphs: time for a new data presentation paradigm. PLoS Biol. 2015; 13: e1002128.

46. ZhengRong Mei, XiangPing Tan, ShaoZhi Liu, HanHui Huang. Puerarin alleviates cognitive impairment and tau hyperphosphorylation in APP/PS1 transgenic mice. Zhongguo Zhong Yao Za Zhi. 2016; 41: 3285-3289.

47. Sevigny J, Chiao P, Bussière T, Weinreb PH, Williams L, Maier M, Dunstan R, Salloway S, et al. The antibody aducanumab reduces Abeta plaques in Alzheimer's disease. Nature. 2016; 537: 50-56.

48. Sneham Tiwari, Venkata Atluri, Ajeet Kaushik, Adriana Yndart, Madhavan Nair. Alzheimer's disease: pathogenesis, diagnostics, and therapeutics. Int J Nanomedicine. 2019; 14: 5541-5554.

49. Enzo Grossi, Andrea Stoccoro, Pierpaola Tannorella, Lucia Migliore, Fabio Coppedè. Artificial neural networks link one-carbon metabolism to gene-promoter methylation in Alzheimer's disease. J Alzheimers Dis. 2016; 53: 1517-1522.

50. Schurr A. Cerebral glycolysis: a century of persistent misunderstanding and misconception. Front Neurosci. 2014; 8: 360.

51. Magistretti PJ, Allaman IA. Cellular perspective on brain energy metabolism and functional imaging. Neuron. 2015; 86: 883-901.

52. Magistretti PJ, Igor Allaman. Lactate in the brain: from metabolic end-product to signalling molecule. Nat Rev Neurosci. 2018; 19: 235-249.